Supporting Information

Solvating Power Series of Electrolyte Solvents for Lithium Batteries

Chi-Cheung Su,[a†] Meinan He,[a†] Rachid Amine,[b] Tomas Rojas,[b,c] Lei Cheng,[b] Anh T. Ngo,[b] and Khalil Amine[a,d*]

[a] Chemical Sciences and Engineering Division, Argonne National Laboratory, 9700 S. Cass Avenue, Lemont, IL 60439, USA

[b] Materials Science Division, Argonne National Laboratory, 9700 S. Cass Avenue, Lemont, IL 60439, USA

[c] Department of Physics and Astronomy and Ohio Materials Institute, Ohio University, Athens, Ohio 45701-2979, USA

[d] Material Science and Engineering, Stanford University, Stanford, CA 94305, USA

[†] *These authors contributed equally to this work.*

E-mail: amine@anl.gov

Table of Contents

Experimental Section

The electrolyte solvent GBL, PC, EC, EA, DMC, EMC, and $LiPF_6$ salt (BASF, battery grade) were used as received. The solvents TFPC, FEMC (MERF facility, Argonne National Laboratory), FEC, and DFEC (Solvay, 99%) were first dehydrated by adding 4 Å molecular sieves and then purified by vacuum distillation before use. Karl-Fischer titration indicated the water content of all solvents was under 20 ppm. Toluene and benzene-d_6 (Sigma-Aldrich, anhydrous) were used as received. All samples were prepared in an argon atmosphere glovebox (<1 ppm of O_2 and H_2O) by mixing the selected molar or volume ratio of each solvent, or by adding an appropriate molar or volume ratio of each solvent to the $LiPF_6$ salt in a vial with stirring until a homogeneous solution was obtained.

Cathode NMC622 ($LiNi_{0.6}Mn_{0.2}Co_{0.2}O_2$) laminates were supplied by the Cell Analysis, Modeling, and Prototyping (CAMP) Facility at Argonne National Laboratory. The electrode laminates were punched into 14 mm discs and dried at 70°C under vacuum overnight.

We performed galvanostatic charge/discharge cycling using 2032 coin cells at a rate of C/2 with a cutoff between 4.4 and 3.0 V following three formation cycles at a rate of C/10. Cell voltage profiles and capacity were recorded using a MACCOR Electrochemical Analyzer. The Li/NMC622 cell used in this work has an NMC622 positive electrode (1.75 mAh cm^{-2} areal capacity), a foil of Li metal anode, one piece of separator (Celgard 2325), and the prepared electrolyte (40 µL in each cell). Both Li/NMC622 and Li/Li coin cells were prepared in an argon atmosphere glovebox (<1 ppm of O_2 and H_2O).

A Li/Cu cell was also prepared in an argon atmosphere glovebox (<1 ppm of O_2 and H_2O). A foil of lithium chip was used as both counter and reference electrodes. The effective area of the Cu foil for Li deposition was 1.60 cm^2, and the volume of electrolyte used in each coin cell was 40 µL. For the cycling test, 2 mAh cm^{-2} of lithium metal was deposited on the Cu foil at 1 mA cm^{-2} current density and then

stripped until the cell potential reached 0.5 V.

Fourier transform infrared (FTIR) studies were conducted on a PerkinElmer Spectrum 100 FT-IT Spectrometer. The FTIR spectra were acquired in the attenuated total reflection mode with 2 cm^{-1} resolution with one scan to avoid evaporation of the volatile solvents, such as DMC and EA. Raman measurements were carried out on a Renishaw inVia Raman Microscope with an exciting laser of 633 nm.

The NMR analyses were carried out on a 300-MHz NMR spectrometer. Deuterated benzene was placed in an external coaxial insert and then in the NMR tube with the samples. The ^{1}H chemical shifts were referenced to benzene-d_6 at 7.16 ppm. All NMR experiments were performed on a 300-MHz spectrometer equipped with a z-axis gradient amplifier and an ATMA BBO probe with a z-axis gradient coil. The maximum gradient strength was 0.214 T/m. Both ^{1}H-DOSY and ^{7}Li-DOSY were performed using the standard dstebpgp3s program, employing a double stimulated echo sequence, bipolar gradient pulses for diffusion, and three spoil gradients. The diffusion time was 200 ms, and the rectangular gradient pulse duration was 1200 μs. Gradient recovery delays were 200 μs. Individual rows of the quasi-2-D diffusion databases were phased and baseline corrected. Actual diffusion coefficients used for the D-α analysis were obtained with commercial software using the T1/T2 analysis module. As representative examples, the ^{1}H-DOSY attenuation curves for toluene, FEC, and EMC in 1:1 FEC:EMC and 1:4:4 (molar ratio) $LiPF_6$:FEC:EMC electrolyte, as well as the ^{7}Li-DOSY attenuation curve for lithium in 1:4:4 (molar ratio) $LiPF_6$:FEC:EMC electrolyte, are shown in Figures S10 through S12.

Density Functional Theory (DFT) methods were used to calculate structures and orbitals of salt-solvent complexes (Hartree-Fock LUMO). B3LYP functional with 6-31+g basis sets as implemented in Gaussian was used to optimize the complex structures.

To calculate the FEMC LUMO levels on both FEC/FEMC and DFEC/FEMC electrolytes, density functional theory (DFT) calculations were performed using the Quantum Espresso software package [1]. We used the exchange-correlation functional developed by Perdew, Burke, and Ernzerhof (PBE) [2] and included dispersion interaction within the D3 correction developed by Grimme et al. [3]. We utilized plane wave pseudopotentials, these plane waves were set with an energy cutoff of 1020 eV, and the

Brillouin zone is sampled using the Γ point. We perform calculations on two different systems representing the electrolytes, these systems are set in a cubic unit cell of 15 A side as seen in Figure S9.

Rationale of IR-DOSY, D-α Analysis and χ Calculation

The electrolyte $LiPF_6$:FEC:EMC 1:4:4 is used below as a representative example to explain the principle of IR-DOSY and D-α analysis.

According to the Stokes-Einstein equation, the diffusion coefficient of FEC in the FEC:EMC 1:1 solution can be described as eq. 1, where T_1 is the temperature, η_1 is the viscosity, k is the Boltzmann constant, and r_1 represents the hydrodynamic radius, the diffusion coefficient is inversely related to the hydrodynamic radius of a molecule.

$$D_{1FEC} = kT_1/6\pi\eta_1 r_1 \qquad \text{eq. 1}$$

When $LiPF_6$ is dissolved in an FEC:EMC 1:1 solution, the lithium cations will be solvated by the solvent molecules. The hydrodynamic radius of FEC and also the viscosity of the solution will increase.

In this study, toluene was added to both FEC:EMC 1:1 solution and $LiPF_6$:FEC:EMC 1:4:4 electrolyte solution as an internal reference. The reasons for using toluene as an internal reference are firstly, unlike other hydrocarbons such as heptane or hexane, the solubility of toluene in polar electrolyte solution is acceptably high (> 5%). Moreover, toluene is a hydrocarbon with remarkably low polarity and donor number. As a result, lithium cations can seldom be solvated by toluene, especially in the presence of polar electrolyte solvents. Therefore, the hydrodynamic radius (r) for toluene should remain unchanged after the addition of lithium salt. As depicted in eq. 2, the ratio of the diffusion coefficients of toluene before and after the addition of $LiPF_6$ (D_{1T} and D_{2T}, respectively) equals $T_1\eta_2/T_2\eta_1$ (T_1 and T_2 are respectively the temperature of the FEC:EMC 1:1 solution before and after the addition of $LiPF_6$, η_1 and η_2 are respectively the viscosity of the FEC:EMC 1:1 solution before and after the addition of $LiPF_6$).

$$\frac{D_{1T}}{D_{2T}} = \frac{\frac{kT_1}{6\pi\eta_1 r}}{\frac{kT_2}{6\pi\eta_2 r}} = \frac{T_1\eta_2}{T_2\eta_1} \qquad \text{eq. 2}$$

Because of the formation of Li^+-FEC complexes, the diffusion coefficient of FEC (D_{2FEC}) is significantly decreased after the addition of $LiPF_6$ due to the increases in both hydrodynamic radius and viscosity. Since the hydrodynamic radius of the non-coordinating FEC molecule should be unchanged after the addition of $LiPF_6$, the diffusion coefficient of non-coordinating free FEC ($D_{free\ FEC}$) in the electrolyte solution can be calculated from eq. 3.

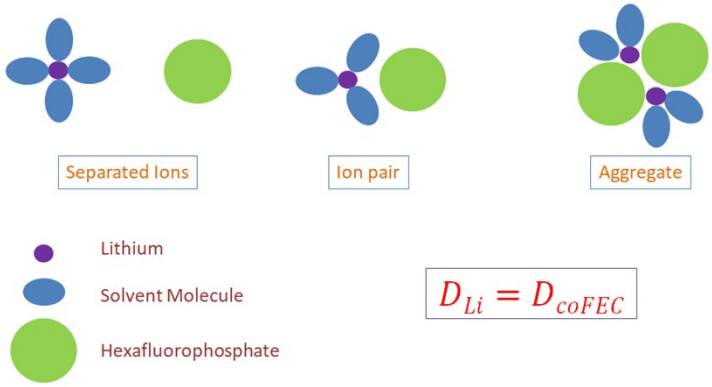

In the $LiPF_6$:FEC:EMC 1:4:4 electrolyte solution, ion pairs or aggregates may also co-exist with solvated separated ions if the lithium salt is not fully dissociated. It is obvious that the lithium in solvated separated ions, ion pairs, or aggregates will also be solvated by the polar electrolyte solvent due to the high Lewis acidity of lithium cation, as depicted above. In contrast, anion in lithium salt such as hexafluorophosphate is barely solvated directly by electrolyte solvent, though it is not uncommon for anions to form ion pairs or aggregates with lithium cations. Thus, it is reasonable to assume that the electrolyte solvent solvating the lithium should present a similar diffusion coefficient as the lithium, as represented in eq. 3. [ref S1]

At room temperature, the ligand exchange process in electrolyte is on a much faster timescale than the acquisition of NMR signals. Therefore, the measured diffusion coefficient of FEC in the salted electrolyte

solution D_{2FEC} is the average of the diffusion coefficients of coordinated FEC ($D_{Co\text{-}FEC}$) and free EMC ($D_{free\ FEC}$) as illustrated in eq. 4, wherein α is the coordination ratio of FEC.

Using eqs. 2 to 5, the coordination percentage of FEC can be calculated.

$$D_{Li} = D_{Co-FEC} \quad \text{eq. 3}$$

$$D_{free\ FEC} = \frac{\frac{kT_1}{6\pi\eta_1 r_1}}{\frac{kT_2}{6\pi\eta_2 r_1}} D_{1FEC} = \frac{T_1\eta_2}{T_2\eta_1} D_{1FEC} \quad \text{eq. 4}$$

$$D_{2FEC} = D_{Co-FEC}\alpha + D_{free\ DME}(1-\alpha) \quad \text{eq. 5}$$

Relative solvating power χ is defined as the ratio between the coordination percentage of a test solvent (α) and the coordination percentage of a reference solvent (α_0) as described in eq. 6. In this study, the reference solvent is EMC and thus, α_0 is α_{EMC}.

$$\chi = \frac{\alpha}{\alpha_0} \quad \text{eq. 6}$$

For $LiPF_6$:FEC:EMC 1:4:4 electrolyte, α_{FEC} is 0.32 and α_{EMC} is 0.51. Therefore, the relative solvating power χ of FEC is 0.63.

Theoretical Calculation on the Decomposition Pathway of FEMC

As a start, we focused on the adsorption of FEMC molecule on a lithium surface. For this purpose, we performed DFT calculations as implemented in the Vienna Ab-initio Software Package (VASP) [S6-S9]. Particularly we used the exchange-correlation developed by Perdew, Burke, and Ernzerhof (PBE) [S2] that included the van der Waals interactions as implemented in the DFT-D3 correction developed by Grimme *et al.* [S3].

These calculations were performed using a plane wave cutoff energy of 600 eV and Brillouin zone sampling using the Γ point. The surface supercell was built using 6 layers of 4x4 Li atoms, and a layer of 25 Å of vacuum is added to minimize interaction between parallel surfaces.

We considered a large variety of possible adsorption configurations for the FEMC molecule over the lithium surface. For each of them electronic optimizations were carried out, as well as for the pristine surface and the isolated molecule. These calculations were performed with a force criterion of 0.01 eV/Å. Before the optimization, the molecules are set at 3 Å from the lithium surface. To evaluate their energetics, we calculated their binding energies which we defined as $\Delta E = E_{mol+surf} - E_{mol} - E_{surf}$, where E_{mol}, E_{surf} and $E_{mol+surf}$ represent the ground state energy of the isolated FEMC molecule, the clean Li (100) surface and the molecule over the surface systems respectively.

According to our results, the lowest energy (-7.27 eV) configuration corresponds to the case shown in Figure S10 in which the carbonyl oxygen in the molecule binds directly on top of the lithium surface. The strength of the interaction between O and Li produces significant distortions in the surface, removing the Li atom from the surface by about 1 Å.

Once the molecule is adsorbed on the Li surface, the transfer of an electron from the surface towards the carbonyl group can trigger different side reactions that can impair the integrity of the compact SEI formed by the reductive decomposition of DFEC.

To explore possible reactions taking place in the decomposition of FEMC molecule, we performed DFT calculations as implemented in the Gaussian 09 package, using the B3LYP functional with 6-31+g* basis set. [S10] We performed optimization in the gas phase for every product and reactant in each reaction and calculated the reaction energy by subtracting the optimized energy levels. In this definition, negative reaction energy represents an energetically favorable reaction.

Figure S11 depicts two major possible decaying pathways for FEMC. The first pathway involves the breaking down of the FEMC radical anion to produce a CF_3CH_2 radical and a CO_3CH_3 anion with favorable reaction energy of 0.51 eV. The methyl carbonate can further decompose into a CO_2 molecule and a methoxide with favorable reaction energy of 1.43 eV, representing the lowest reaction energy of all cases considered. Secondly, the FEMC molecule can break down into a CH_3 radical and a $CF_3CH_2CO_3$ anion with favorable reaction energy of 0.97 eV. The trifluoroethyl carbonate can be further

decarboxylated to form a CO_2 molecule and trifluoroethoxide with a 1.53 eV energy barrier. However, the reaction energy is based on the gas phase calculation mentioned above and in reality, the generation of carbon dioxide gas can provide significant entropy drive of the reaction. Apparently, the first pathway gives the thermodynamic products while the second pathway generates the kinetic products. The methoxide and trifluoroethoxide can easily nucleophilically attack the carbonate solvents, resulting in the formation of different by-products such as polycarbonate and polyethylene glycol. The presence of a significant amount of these by-products can impair the compact SEI formed by the reductive decomposition of DFEC.

The presence of radicals, carbanions and radical anions are common and have been proposed for similar compounds such as diethyl carbonate and dimethyl carbonate along with production of CO_2 in lithium ion batteries. [S11]

Reference:

Ref [S1] P. Giannozzi, S. Baroni, N. Bonini, M. Calandra, R. Car, C. Cavazzoni, D. Ceresoli, G.L. Chiarotti, M. Cococcioni, I. Dabo, A.D. Corso, S. Fabris, G. Fratesi, S. de Gironcoli, R. Gebauer, U. Gerstmann, C. Gougoussis, A. Kokalj, M. Lazzeri, L. Martin-Samos, N. Marzari, F. Mauri, R. Mazzarello, S. Paolini, A. Pasquarello, L. Paulatto, C. Sbraccia, S. Scandolo, G. Sclauzero, A.P. Seitsonen, A. Smogunov, P. Umari, and R.M. Wentzcovitch, *J. Phys. Condens. Matter* **21**, 395502 (2009).
Ref [S2] J.P. Perdew, K. Burke, and M. Ernzerhof, *Phys. Rev. Lett*. 77, 3865 (**1996**).
Ref [S3] S. Grimme et al., *J. Chem. Phys*. 132, 154104 (**2010**).
Ref [S4]. Su, C.-C.; He, M.; Amine, R.; Chen, Z.; Amine, K. *J. Phys. Chem. Lett*., **2018**, *9* (13), 3714.
Ref [S5]. Su, C.-C.; He, M.; Amine, R.; Chen, Z.; Amine, K., *Angewandte Chemie* **2018**, 57 (37), 12033.
Ref [S6] G. Kresse and J. Hafner. *Phys. Rev. B*, 47:558, **1993**.
Ref [S7] G. Kresse and J. Hafner. *Phys. Rev. B*, 49:14251, **1994**.
Ref [S8] G. Kresse and J. Furthmüller. Comput. *Mat. Sci*., 6:15, **1996**.
Ref [S9] G. Kresse and J. Furthmüller. *Phys. Rev. B*, 54:11169, **1996**.
Ref [S10] M. J. Frisch, G. W. Trucks, H. B. Schlegel, G. E. Scuseria, M. A. Robb, J. R. Cheeseman, G. Scalmani, V. Barone, B. Mennucci, G. A. Petersson, H. Nakatsuji, M. Caricato, X. Li, H. P. Hratchian, A. F. Izmaylov, J. Bloino, G. Zheng and J. L. Sonnenberg, Gaussian 09, **2009**.
Ref [S11] Seo, D. M.; Chalasani, D.; Parimalam, B. S.; Kadam, R.; Nie, M.; Lucht, B. L.,. *ECS Electrochemistry Letters* **2014**, *3 (9)*, A91-A93.

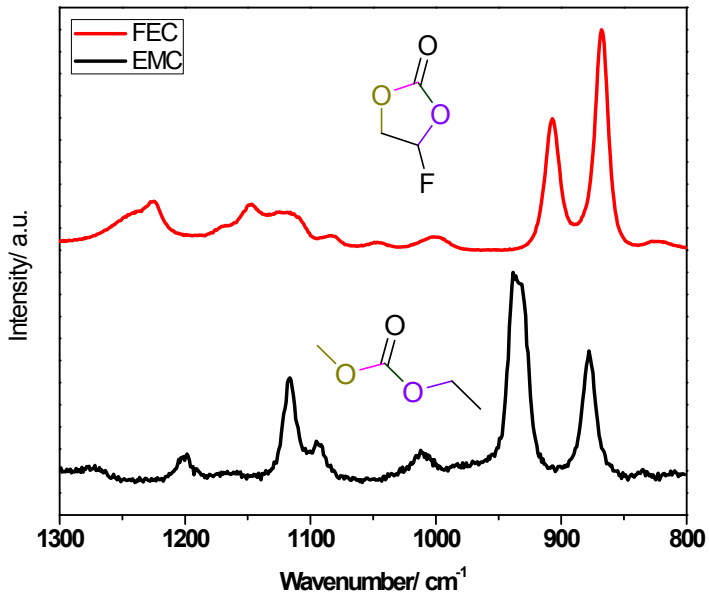

Figure S1. Raman spectra of C-O groups in FEC and EMC.

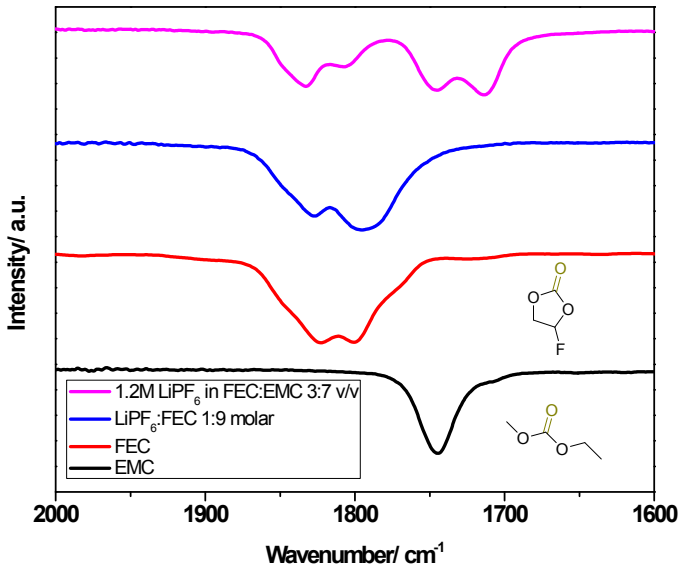

Figure S2. FTIR spectra of C=O groups in FEC, EMC, $LiPF_6$:FEC 1:9 (molar) and 1.2 M $LiPF_6$ in FEC:EMC 3:7 v/v solution.

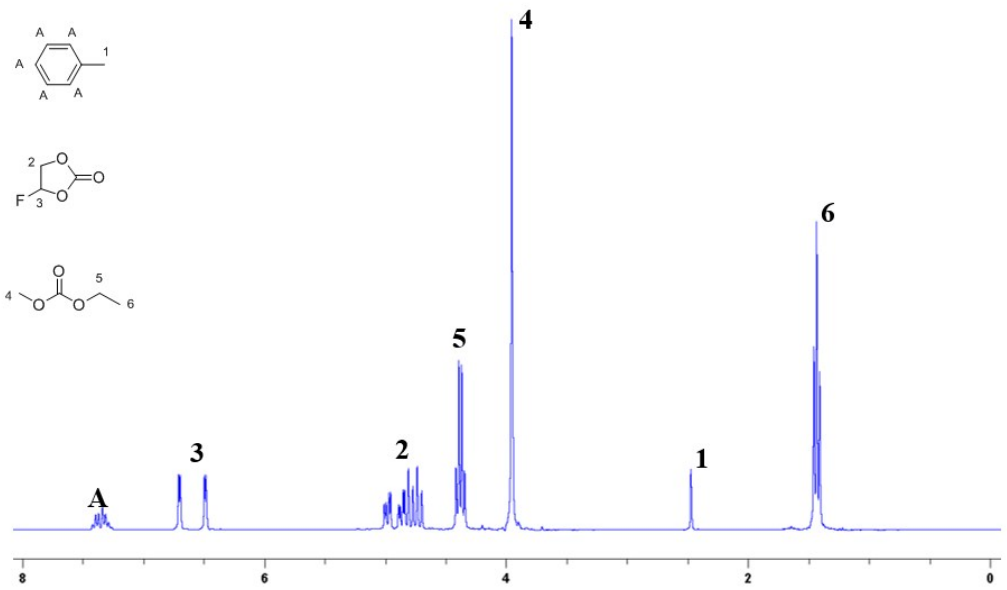

Figure S3. ^{1}H NMR spectrum of $LiPF_6$:FEC:EMC 1:4:4 solution with toluene added as internal reference.

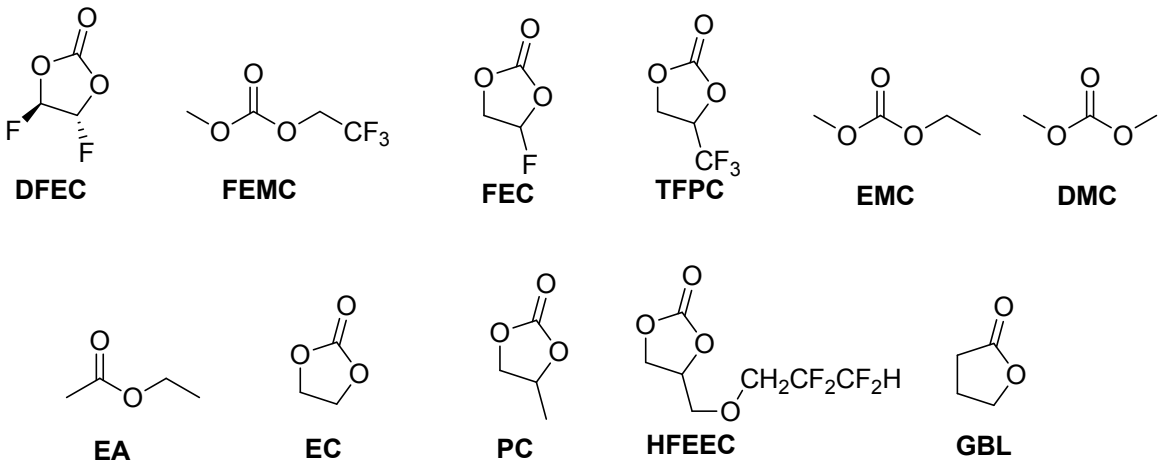

Figure S4. Chemical structures of DFEC, FEMC, FEC, TFPC, EMC, DMC, EA, EC, PC, HFEEC, and GBL.

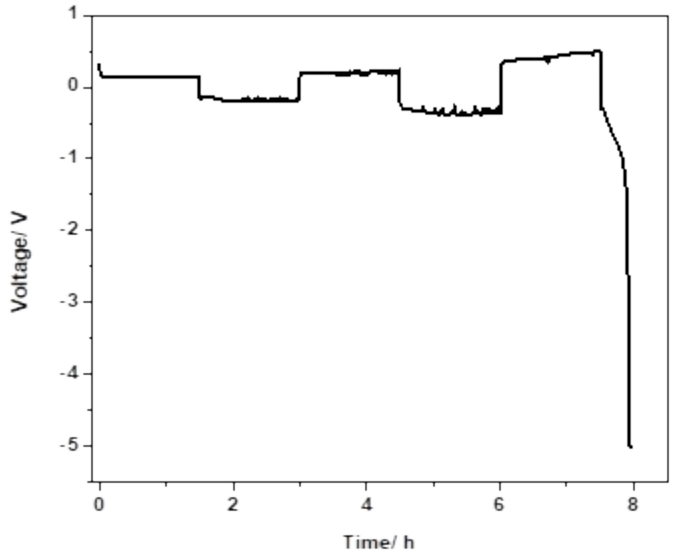

Figure S5. Voltage profiles for Li/Li symmetric cells cycled at 2 $mAcm^{-2}$ with 1.2 M $LiPF_6$ FEMC.

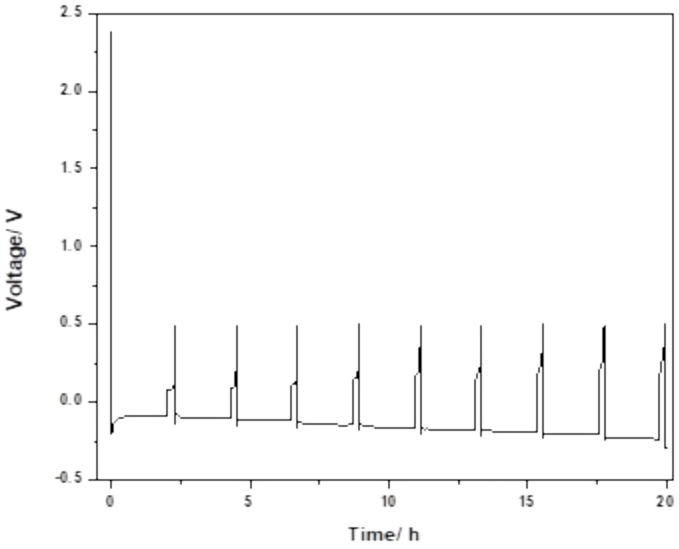

Figure S6. Electrochemical performance of Li plating/striping using Li/Cu cells cycled at 1 mA cm^{-2} with 1.2 M $LiPF_6$ FEMC.

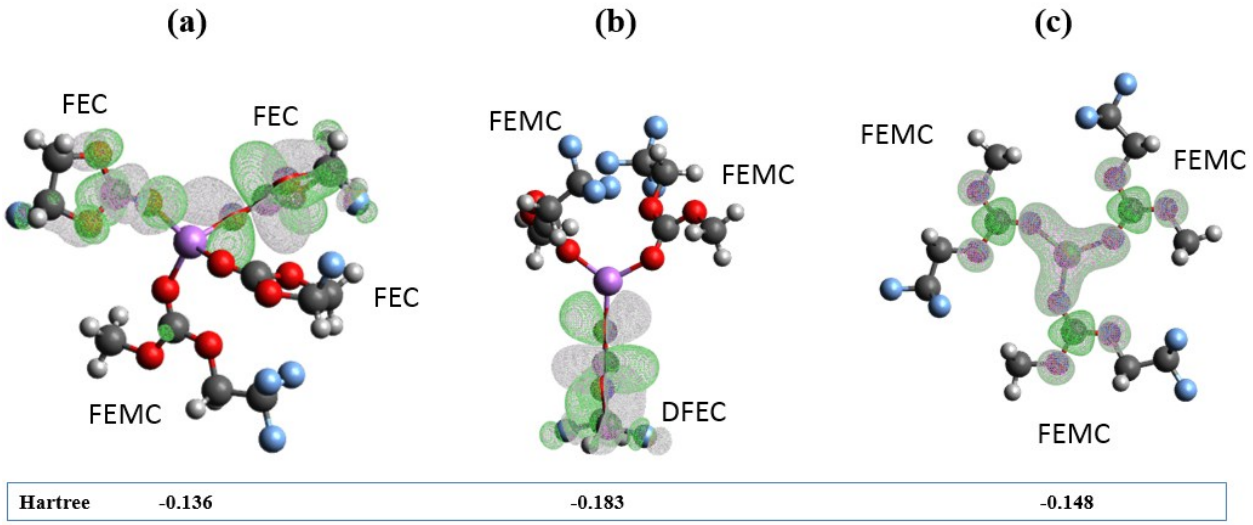

Hartree	-0.136	-0.183	-0.148

Figure S7. LUMO of (a) $Li^+(FEC)_3(FEMC)$, (b) $Li^+(DFEC)(FEMC)_2$ and (c) $Li^+(FEMC)_3$.

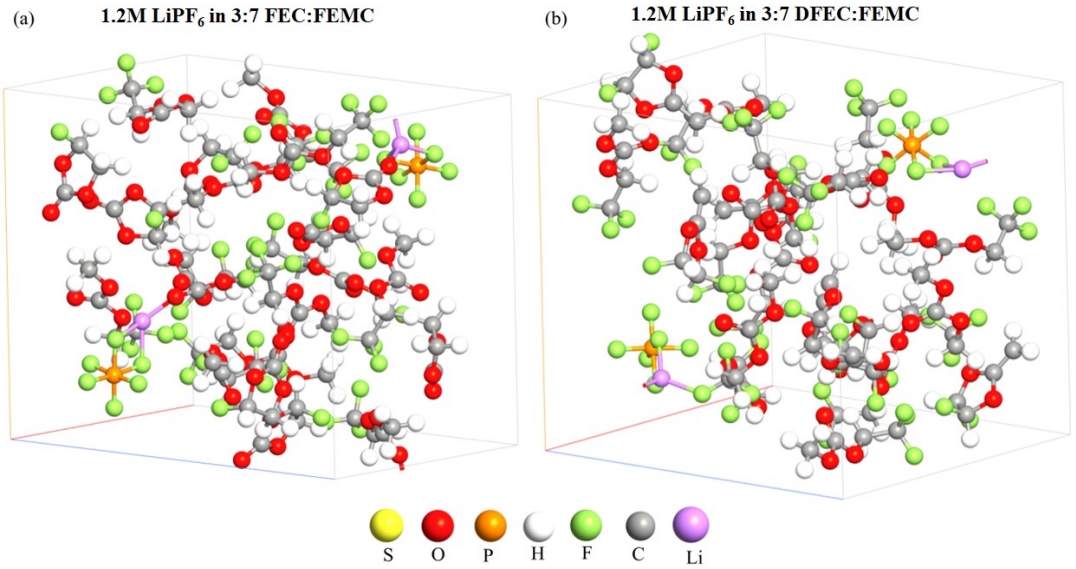

Figure S8. Unit cell representing 1.2M $LiPF_6$ in (a) volume ratio 3:7 FEC:FEMC and (b) volume ratio 3:7 DFEC:FEMC electrolytes. These structures are the result from variable volume electronic relaxation.

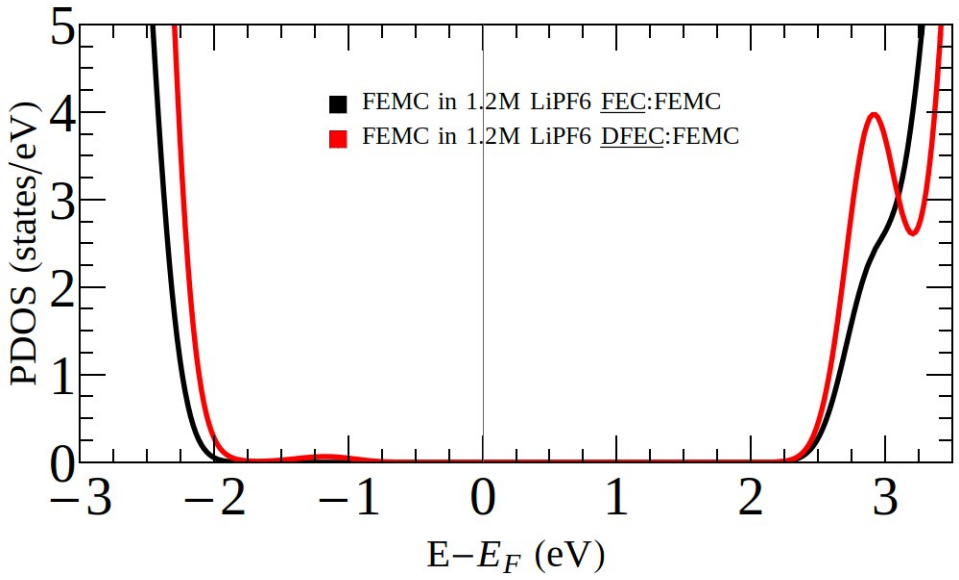

Figure S9. Projected density of states (PDOS) of FEMC obtained in DFT simulations on 1.2 M $LiPF_6$ FEC:FEMC 3:7 and 1.2 M $LiPF_6$ DFEC:FEMC 3:7 electrolytes.

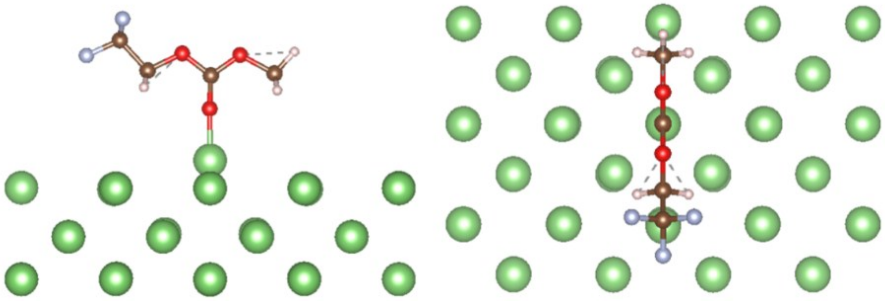

Figure S10. Top and side view of the coordinates of the FEMC molecule adsorbed over on the Li (100) surface. This configuration has a binding energy of -7.27 eV. In this case, green, brown, gray and pink represent lithium, carbon, fluorine, and hydrogen respectively.

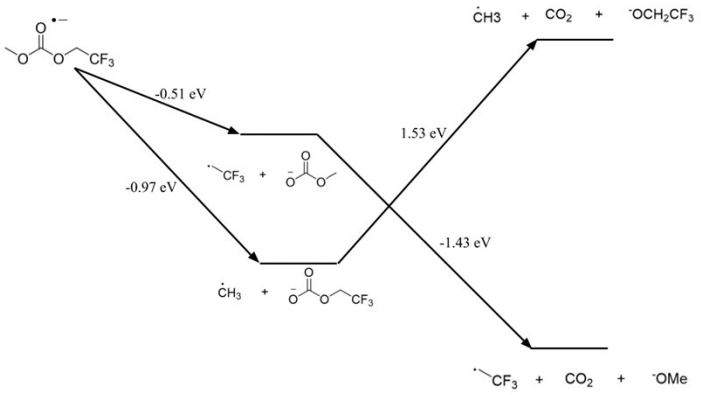

Figure S11. Energy diagram of the possible reactions taking part in the decomposition of FEMC molecule.

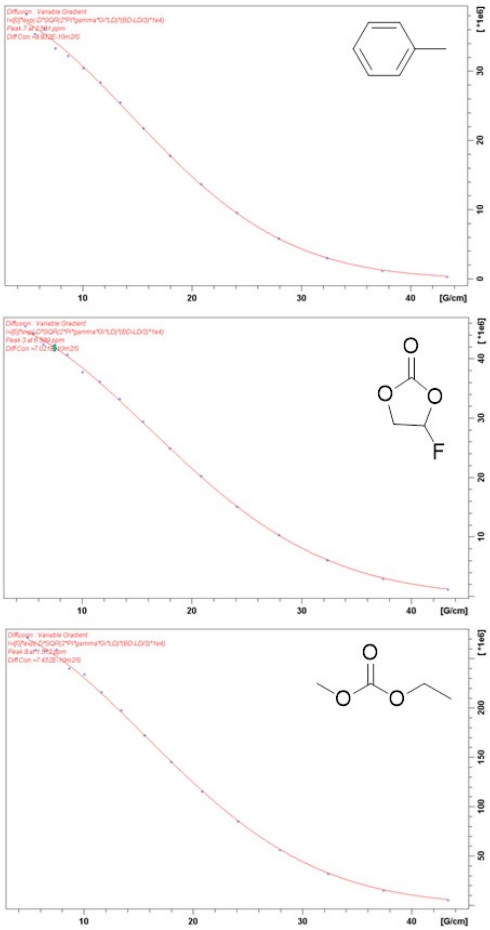

Figure S12. ^{1}H DOSY attenuation curves for toluene, FEC and EMC in 1:1 FEC:EMC.

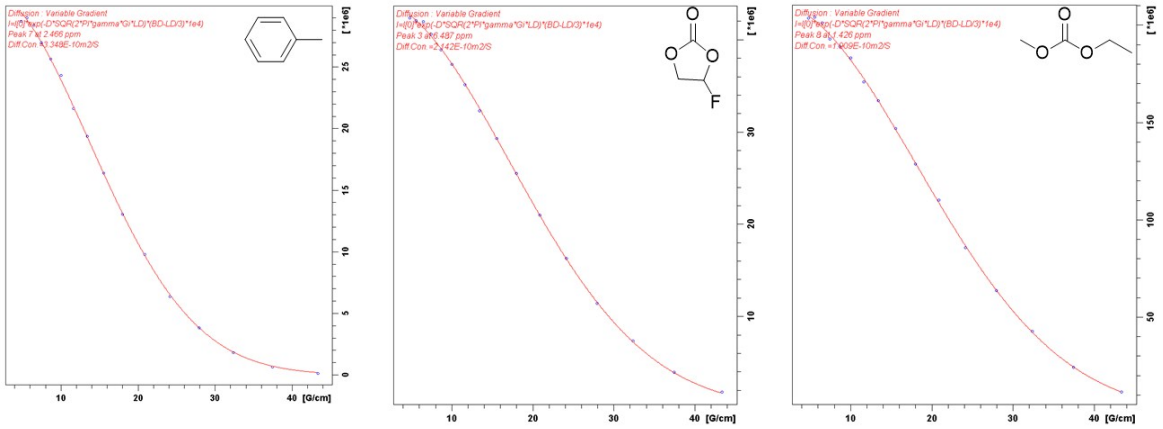

Figure S13. ^{1}H DOSY attenuation curves for toluene, FEC, and EMC in 1:4:4 $LiPF_6$:FEC:EMC.

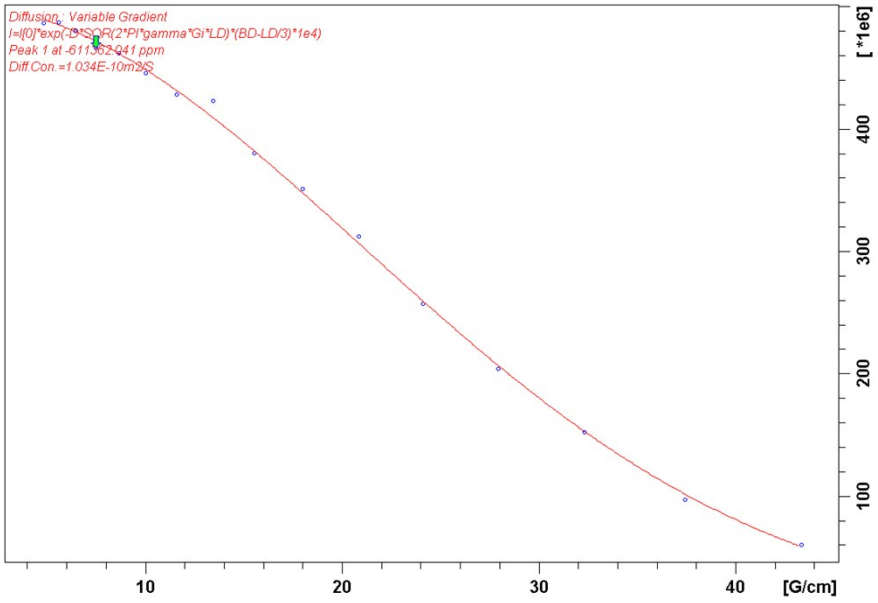

Figure S14. ^{7}Li DOSY attenuation curve for lithium in 1:4:4 $LiPF_6$:FEC:EMC.

Table S1. Coordination ratio α and coordination number of 1:4:4 $LiPF_6$:FEC:EMC electrolyte.

Solution	D_{Tol}[a]	D_{FEC}[a]	D_{EMC}[a]	D_{Li}[a]	α_{FEC}	α_{EMC}	Coordination number of Li[b]
1:1 FEC:EMC	8.83	7.02	7.45	N/A	N/A	N/A	N/A
1:4:4 $LiPF_6$:FEC:EMC	3.35	2.14	1.91	1.03	0.32	0.51	3.31

[a] Diffusion coefficients in units of 10^{-10} m^2/s.

[b] Coordination number of Li was calculated by multiplying the coordination ratios of electrolyte solvents with their molar ratios.

Table S2. Coordination ratio α and coordination number of 1:4:4 $LiPF_6$:DFEC:EMC electrolyte.

Solution	D_{Tol}[a]	D_{DFEC}[a]	D_{EMC}[a]	D_{Li}[a]	α_{DFEC}	α_{EMC}	Coordination number of Li[b]
1:1 DFEC:EMC	10.8	8.75	8.95	N/A	N/A	N/A	N/A
1:4:4 $LiPF_6$:DFEC:EMC	4.28	3.33	2.13	1.53	0.07	0.72	3.16

[a] Diffusion coefficients in units of 10^{-10} m^2/s.

[b] Coordination number of Li was calculated by multiplying the coordination ratios of electrolyte solvents with their molar ratios.

Table S3. Coordination ratio α and coordination number of 1:4:4 $LiPF_6$:FEMC:EMC electrolyte.

Solution	D_{Tol}[a]	D_{FEMC}[a]	D_{EMC}[a]	D_{Li}[a]	α_{FEMC}	α_{EMC}	Coordination number of Li[b]
1:1 FEMC:EMC	14.3	11.2	12.9	N/A	N/A	N/A	N/A
1:4:4 $LiPF_6$:FEMC:EMC	6.96	4.70	4.07	2.55	0.26	0.59	3.42

[a] Diffusion coefficients in units of 10^{-10} m^2/s.

[b] Coordination number of Li was calculated by multiplying the coordination ratios of electrolyte solvents with their molar ratios.

Table S4. Coordination ratio α and coordination number of 1:4:4 $LiPF_6$:TFPC:EMC electrolyte.

Solution	D_{Tol}[a]	D_{TFPC}[a]	D_{EMC}[a]	D_{Li}[a]	α_{TFPC}	α_{EMC}	Coordination number of Li[b]
1:1 TFPC:EMC	7.92	5.30	6.78	N/A	N/A	N/A	N/A
1:4:4 $LiPF_6$:TFPC:EMC	3.27	1.64	1.82	1.08	0.47	0.57	4.18

[a] Diffusion coefficients in units of 10^{-10} m^2/s.

[b] Coordination number of Li was calculated by multiplying the coordination ratios of electrolyte solvents with their molar ratios.

Table S5. Coordination ratio α and coordination number of 1:4:4 $LiPF_6$:DMC:EMC electrolyte.

Solution	D_{Tol}[a]	D_{DMC}[a]	D_{EMC}[a]	D_{Li}[a]	α_{DMC}	α_{EMC}	Coordination number of Li[b]
1:1 DMC:EMC	16.6	17.2	15.8	N/A	N/A	N/A	N/A
1:4:4 $LiPF_6$:DMC:EMC	7.75	5.24	4.95	2.51	0.51	0.50	4.02

[a] Diffusion coefficients in units of 10^{-10} m^2/s.

[b] Coordination number of Li was calculated by multiplying the coordination ratios of electrolyte solvents with their molar ratios.

Table S6. Coordination ratio α and coordination number of 1:4:4 $LiPF_6$:EA:EMC electrolyte.

Solution	D_{Tol}[a]	D_{EA}[a]	D_{EMC}[a]	D_{Li}[a]	α_{EA}	α_{EMC}	Coordination number of Li[b]
1:1 EA:EMC	19.1	20.2	18.4	N/A	N/A	N/A	N/A
1:4:4 $LiPF_6$:EA:EMC	9.34	6.20	6.27	2.04	0.53	0.45	3.95

[a] Diffusion coefficients in units of 10^{-10} m^2/s.

[b] Coordination number of Li was calculated by multiplying the coordination ratios of electrolyte solvents with their molar ratios.

Table S7. Coordination ratio α and coordination number of 1:4:4 $LiPF_6$:EC:EMC electrolyte.

Solution	D_{Tol}[a]	D_{EC}[a]	D_{EMC}[a]	D_{Li}[a]	α_{EC}	α_{EMC}	Coordination number of Li[b]
1:1 EC:EMC	9.76	8.93	9.00	N/A	N/A	N/A	N/A
1:4:4 $LiPF_6$:EC:EMC	3.60	1.97	2.37	1.33	0.68	0.48	4.61

[a] Diffusion coefficients in units of 10^{-10} m^2/s.

[b] Coordination number of Li was calculated by multiplying the coordination ratios of electrolyte solvents with their molar ratios.

Table S8. Coordination ratio α and coordination number of 1:4:4 $LiPF_6$:PC:EMC electrolyte.

Solution	D_{Tol}[a]	D_{PC}[a]	D_{EMC}[a]	D_{Li}[a]	α_{PC}	α_{EMC}	Coordination number of Li[b]
1:1 PC:EMC	10.5	8.31	9.83	N/A	N/A	N/A	N/A
1:4:4 $LiPF_6$:PC:EMC	4.06	2.15	2.80	1.62	0.67	0.46	4.52

[a] Diffusion coefficients in units of 10^{-10} m^2/s.

[b] Coordination number of Li was calculated by multiplying the coordination ratios of electrolyte solvents with their molar ratios.

Table S9. Coordination ratio α and coordination number of 1:4:4 $LiPF_6$:HFEEC:EMC electrolyte.

Solution	D_{Tol}[a]	D_{HFEEC}[a]	D_{EMC}[a]	D_{Li}[a]	α_{HFEEC}	α_{EMC}	Coordination number of Li[b]
1:1 HFEEC:EMC	3.17	1.31	2.84	N/A	N/A	N/A	N/A
1:4:4 $LiPF_6$:HFEEC:EMC	1.07	0.27	0.67	0.20	0.69	0.38	4.25

[a] Diffusion coefficients in units of 10^{-10} m^2/s.

[b] Coordination number of Li was calculated by multiplying the coordination ratios of electrolyte solvents with their molar ratios.

Table S10. Coordination ratio α and coordination number of 1:4:4 $LiPF_6$:GBL:EMC electrolyte.

Solution	D_{Tol}[a]	D_{GBL}[a]	D_{EMC}[a]	D_{Li}[a]	α_{GBL}	α_{EMC}	Coordination number of Li[b]
1:1 GBL:EMC	11.2	10.8	10.8	N/A	N/A	N/A	N/A
1:4:4 $LiPF_6$:GBL:EMC	4.56	2.52	3.41	1.41	0.65	0.33	3.93

[a] Diffusion coefficients in units of 10^{-10} m^2/s.

[b] Coordination number of Li was calculated by multiplying the coordination ratios of electrolyte solvents with their molar ratios.

Table S11. Coordination ratio α and coordination number of 1:4:4 $LiPF_6$:FEC:FEMC electrolyte.

Solution	D_{Tol}[a]	D_{FEC}[a]	D_{FEMC}[a]	D_{Li}[a]	α_{FEC}	α_{FEMC}	Coordination number of Li[b]
1:1 FEC:FEMC	6.87	5.63	5.35	N/A	N/A	N/A	N/A
1:4:4 $LiPF_6$:FEC:FEMC	2.83	1.50	1.60	0.84	0.56	0.44	3.99

[a] Diffusion coefficients in units of 10^{-10} m^2/s.

[b] Coordination number of Li was calculated by multiplying the coordination ratios of electrolyte solvents with their molar ratios.

Table S12. Coordination ratio α and coordination number of 1:4:4 $LiPF_6$:DFEC:FEMC electrolyte.

Solution	D_{Tol}[a]	D_{DFEC}[a]	D_{FEMC}[a]	D_{Li}[a]	α_{DFEC}	α_{FEMC}	Coordination number of Li[b]
1:1 DFEC:FEMC	8.82	7.35	6.74	N/A	N/A	N/A	N/A
1:4:4 $LiPF_6$:DFEC:FEMC	3.71	2.80	1.91	0.91	0.13	0.48	2.45

[a] Diffusion coefficients in units of 10^{-10} m^2/s.

[b] Coordination number of Li was calculated by multiplying the coordination ratios of electrolyte solvents with their molar ratios.

Table S13. Relative solvating power of common electrolyte solvents.

Electrolyte solvents	Relative solvating power (χ)[a]
DFEC	0.10
FEMC	0.44
FEC	0.63
TFPC	0.83
EMC	1
DMC	1.02
EA	1.17
EC	1.41
PC	1.46
HFEEC	1.82
GBL	1.95

[a] Relative solvating power (χ) = coordination ratio of electrolyte solvent (α_{ES}) /coordination ratio of EMC (α_{EMC}).